

Fundamental Aspects of Ultrathin Dielectrics on Si-based Devices

Edited by

Eric Garfunkel, Evgeni Gusev
and Alexander Vul'

NATO Science Series

3. High Technology – Vol. 47

Fundamental Aspects of Ultrathin Dielectrics on Si-based Devices, pp. 89-102
Edited by E. Garfunkel, E. Gusev and A. Vul
© Kluwer, Dordrecht, 1997

CORE-LEVEL SHIFTS IN Si(001)-SiO₂ SYSTEMS: THE VALUE OF FIRST-PRINCIPLE INVESTIGATIONS

ALFREDO PASQUARELLO^{1,2,3}, MARK S. HYBERTSEN³,
G.-M. RIGNANESE^{1,4} AND ROBERTO CAR^{1,2}

¹ *Institut Romand de Recherche Numérique en Physique des Matériaux (IRRMA),
Ecublens, CH-1015 Lausanne, Switzerland*

² *Department of Condensed Matter Physics,
University of Geneva, CH-1211 Geneva, Switzerland,*

³ *Bell Laboratories, Lucent Technologies,
700 Mountain Avenue, Murray Hill, New Jersey 07974, USA,*

⁴ *Unité de Physico-Chimie et de Physique des Matériaux,
Université Catholique de Louvain,*

1 Place Croix du Sud, B-1348 Louvain-la-Neuve, Belgium.

Abstract. A first-principle approach allows the study of relaxed structural models for surfaces and interfaces. This is a powerful tool for the study of the local bonding. The utility of the first-principle theory is substantially extended through the calculation of core-level shifts. Such results can be used in conjunction with measured photoemission spectra to make progress in understanding the local atomic structure at interfaces. We review the quantitative comparison of the calculated core level shifts with experiment for a series of molecules. We then describe results for the Si(001)-SiO₂ interface.

1. Introduction

Core-level photoemission spectroscopy stands out as one of the most successful tools for providing direct information on the local bonding environment of specific atoms at surfaces and interfaces. The interpretation of photoemission spectra is often straightforward, and comparison with molecular counterparts or simple charge-transfer models appear to be sufficient

to extract the relevant structural information. However, in some cases core-hole relaxation effects are sizeable and cannot be neglected. Furthermore, at surfaces and interfaces, the bonding environments may differ significantly from those in molecular counterparts, making quantitative predictions of core-level shifts as deduced from molecular analogs very difficult. Because of these reasons, the availability of a reliable theoretical framework could represent an invaluable tool for the assignment of unidentified spectral features.

First-principle approaches in which the electronic structure is described within density functional theory (DFT) could serve this purpose [1, 2]. Such approaches have several advantages. Because the forces acting on the ions can also be calculated within these approaches [3, 4], a structural optimization can be performed, providing in this way reasonable configurational models even when the actual structures are unknown. Then, core-level shifts, including core-hole relaxation effects, can be evaluated consistently within the same theoretical framework. An additional advantage of this approach derives from the fact that core-shifts are sensitively affected only by modifications of the electronic structure in the valence band. Such changes can accurately be described within a pseudopotential approach in which only valence electrons are treated explicitly [5]. This in turn allows the application of this approach to relatively large systems containing up to a hundred atoms given the current computational means.

The purpose of this work is to assess the current status of this theoretical method by describing its merits and its limitations in a series of applications. These range from small molecules to more complex systems such as surfaces and interfaces. More specifically, we focus here on core-level shifts induced by adsorbates forming Si-O bonds on Si(001) surfaces and on the relation between core-level shifts and bonding environments at Si(001)-SiO₂ interfaces.

This paper is organized as follows. A brief description of our approach for calculating core-level shifts is given in Section 2. In Section 3, a comparison between calculated and measured core-level shifts in a series of molecules provides a quantitative measure of the degree of accuracy that can be achieved with this approach. In Section 4, we calculate the shifts induced by dissociated water and spherosiloxane molecules on Si(001) surfaces. In Section 5, calculated Si 2*p* core-level shifts for all the different oxidation states of silicon at Si(001)-SiO₂ interfaces are presented. Finally, in Section 6, we apply our approach to nitrated Si(001)-SiO₂ interfaces and establish a relation between the N 1*s* core-level shifts and the bonding configurations of the incorporated N atoms.

2. Theoretical approach

The atomic relaxations and the core-shift calculations were performed within the local density approximation (LDA) to DFT [6]. Our approach accounts for the electronic structure and consistently provides atomic forces [3, 4]. Only valence electrons are explicitly considered using pseudopotentials (PPs) to account for core-valence interactions. The core-level shifts can be calculated both within the initial state approximation and including core-hole relaxation [7, 2]. The difficulty of using a PP approach is overcome as follows. Initial-state shifts are obtained in first order perturbation theory by evaluating the expectation value of the local potential on the atomic core-orbital, while final state effects are included by considering differences in total energies [5]. Following these procedures *relative* core-level shifts can be determined. Throughout this paper, we only considered vertical excitations, i.e. the molecular structure in the final state is the same as in the initial state. A detailed description of our approach is given in Refs. [7, 2].

3. Small molecules

The accuracy of LDA-DFT for the calculation of core-level shifts [1, 2, 8] can be examined by considering a series of small molecules for which experimental data are available [9]. We considered small molecules containing Si and N atoms. After full relaxation of the molecular structures, we calculated Si 2*p* and N 1*s* core-level shifts both in the initial-state approximation and including core-hole relaxation. The calculated shifts are reported in Table 1 and Table 2, together with the experimental results. The technical aspects of these calculations are given in Refs. [2, 8].

Overall agreement between theory and experiment is very good. In Table 1, the linear additivity of the shifts observed in the experimental data is also found in the calculated values. Another significant case is that of Si(CH₃)₄. On the grounds of simple electronegativity arguments a negative Si 2*p* shift is expected. However, the experimental shift is positive and theory correctly reproduces it. For molecules in which the neighboring atoms to the excited silicon atoms are hydrogen, silicon, chlorine or carbon atoms the error is smaller than a few tenths of an eV.

The necessity of considering core-hole relaxation effects appears more evidently in the case of the N 1*s* shifts given in Table 2. The agreement with experiment of these shifts is noticeably improved when final states are accounted for. In the N series, theoretical and experimental shifts differ by less than 0.3 eV over a broad range of shifts.

This level of accuracy is not found for the Si 2*p* shifts of molecules containing oxygen atoms: O(SiH₃)₂, O(SiCl₃)₂ and Si(OCH₃)₄. Although the

TABLE 1. Relative Si $2p$ initial-state and full shifts for a series of molecules. Experiment from [9]. Shifts are in eV. Negative shifts indicate higher binding energies.

	Initial State	Full	Expt.
SiH ₄	0.00	0.00	0.00
Si ₂ H ₆	-0.03	0.47	0.42
SiClH ₃	-0.88	-0.95	-0.83
SiCl ₂ H	-2.28	-2.45	-2.16
SiCl ₄	-2.89	-3.13	-3.11
O(SiH ₃) ₂	-0.42	-0.79	-0.53
O(SiCl ₃) ₂	-2.75	-3.24	-2.86
Si(CH ₃) ₄	1.00	1.21	1.32
SiH ₃ CH ₃	0.31	0.40	0.46
SiCl ₃ CH ₃	-1.97	-2.10	-1.97
SiH ₂ ClCH ₃	-0.55	-0.54	-0.48
Si(OCH ₃) ₄	-0.15	-1.67	-0.42

TABLE 2. Same as in Table 1, but for N $1s$ core-level shifts.

	Initial State	Full	Expt.
NH ₃	0.00	0.00	0.0
NH ₂ CH ₃	0.06	0.57	0.5
NH(CH ₃) ₂	-0.08	0.58	0.7
N(CH ₃) ₃	-0.33	0.61	0.8
NH ₂ COH	-1.73	-1.13	-0.8
NO ₂	-6.91	-7.24	-7.3
N ₂ O (N*NO)	-3.46	-3.30	-3.1
(NN*O)	-6.77	-7.08	-7.0
CINO	-6.53	-5.68	-5.8

calculated shifts for these three molecules still show the correct qualitative trend, a quantitative discrepancy is observed. Calculated Si $2p$ core-shifts of silicon atoms which have oxygen neighbors, systematically overestimate the shifts towards larger binding energies relative to experiment. Using linear additivity arguments, one can estimate the excess negative shift to be about -0.3 eV per oxygen neighbor.

These results together with similar results obtained for C $1s$ shifts [1]

confirm that LDA-DFT is overall quite successful in reproducing the observed core-level shifts. In the particular case of Si $2p$ core-level shifts in the presence of oxygen neighbors, the difference with experiment has been demonstrated to be systematic. This therefore allows useful conclusions even in these cases as we illustrate in the following sections.

4. Adsorbates on Si(001) interfaces

In this section, we consider dissociated water and spherosiloxane molecules on Si(001) surfaces, which are two different adsorbates forming Si-O bonds with the surface. The former gives rise to a well understood microscopic structure and therefore allows a stringent comparison between theory and experiment [10]. The microscopic structure resulting from the adsorption of spherosiloxane molecules can only be hypothesized by comparison with similar chemical reactions [11, 12]. In this case, the application of our approach allows one to critically examine the proposed structural model by comparison with experimental spectra [13].

4.1. DISSOCIATED WATER MOLECULES ON Si(001)

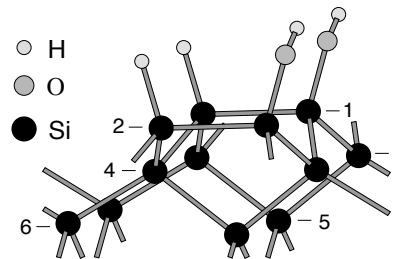


Figure 1. Ball and stick model of the relaxed positions resulting from dissociative water adsorption on Si(001). Distinct Si positions are labelled.

It is by now well established that H₂O is adsorbed dissociatively on Si(001)2×1 by saturating the free dangling bonds of the clean surface with $-OH$ and $-H$ groups [14]. In Fig. 1, we show the structure that results from our structural optimization process [10]. The Si $2p$ shift of the Si atom (1) directly bonded to the $-OH$ group is found to be -1.1 eV with respect to the bulk value [10]. This compares rather well with the measured shifts of -1.0 eV (Ref. [15]) and -0.9 eV (Ref. [16]). The slight overestimation should be related to the same systematic effect as observed in the molecules. Core-hole relaxation is crucial to obtain this agreement, since the initial

state shift calculated for the Si atom (1) is only -0.5 eV. The full shifts of the other Si atoms [(2) to (6)] are all within 0.2 eV from the bulk value. This agreement further strengthens the reliability of our theoretical approach.

4.2. DISSOCIATED SPHEROSILOXANE MOLECULES ON Si(001)

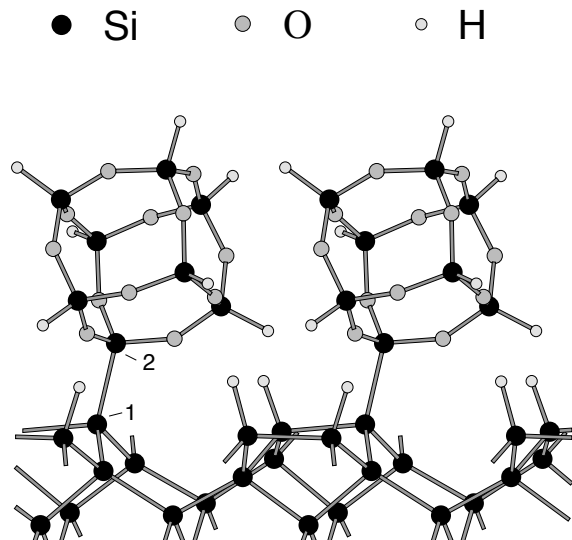


Figure 2. Ball and stick model of the relaxed surface structure of chemisorbed $H_8Si_8O_{12}$ clusters on Si(001).

In Fig. 2, we show the relaxed configuration corresponding to a spherosiloxane ($H_8Si_8O_{12}$) molecule attached at the surface through dissociation of one of its Si-H bonds [13]. This structural model was presumed for the experimental assignment of peaks in the measured photoemission spectrum corresponding to the new interface structure resulting from spherosiloxane clusters and Si(001) [11, 12]. In particular, in the experiment Si $2p$ peaks were observed at -1.04 eV and at -2.19 eV [11]. These peaks were attributed to the substrate silicon atom (1) and the cluster atom (2), respectively. Such assignments radically contrast with the more traditional interpretation which attributes a shift of approximately -1 eV for every nearest-neighbor oxygen atom [16–18]. Si atoms (1) and (2) would be in a Si^0 and Si^{+3} oxidation state with expected shifts of ≈ 0 and ≈ -3 eV, respectively.

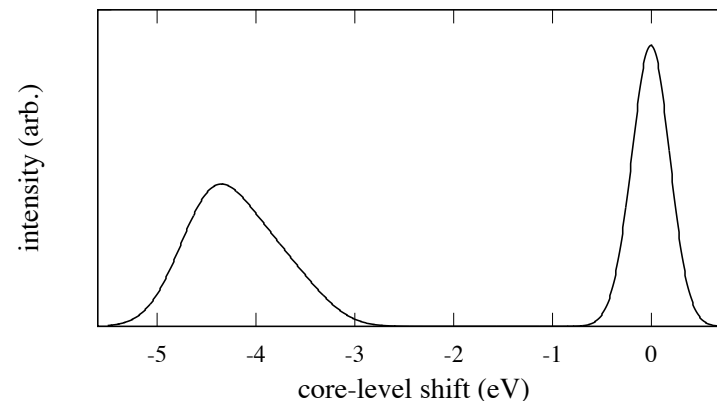


Figure 3. Calculated Si $2p$ core-level spectrum for chemisorbed $H_8Si_8O_{12}$ clusters on Si(001), corresponding to the model structure shown in Fig. 2. The relative intensities of the two peaks are arbitrary.

The calculated Si $2p$ shifts [13] for the model in Fig. 2 are represented schematically in Fig. 3, in which a Gaussian broadening was introduced to account for dynamical effects: a FWHM of 0.4 eV for Si^0 and 0.7 eV for Si^{+3} . All the Si^0 atoms merge in a single peak which coincides with the bulk reference peak. The Si^{+3} atoms belonging to the cluster give rise to an asymmetric peak with a maximum at -4.3 eV and with a FWHM of 1.1 eV. This peak agrees well with the experimental spectrum, where at high binding energies a well defined peak is found at -3.64 eV with a FWHM of 1.2 eV. The overestimation is again attributed to the systematic effect observed in Si-O systems. The asymmetric shape of the high-energy peak results from core-hole relaxation which depends on distance to the screening silicon substrate. This calculation shows that the presumed model cannot account for the experimentally observed peaks at -1.04 eV and at -2.19 eV, and suggest that the actual interface formed by spherosiloxane molecules and Si(001) is more complex.

5. The Si(001)-SiO₂ interface

Photoemission spectra indicate that the three intermediate oxidation states of silicon occur in roughly comparable amounts at the Si(001)-SiO₂ interface [16–18]. We generated several structural models of this interface with the minimal transition region required to be consistent with the photoemission data [7, 19, 20]. Further constraints come from electrical measurements which indicate the presence of an extremely low density of defects

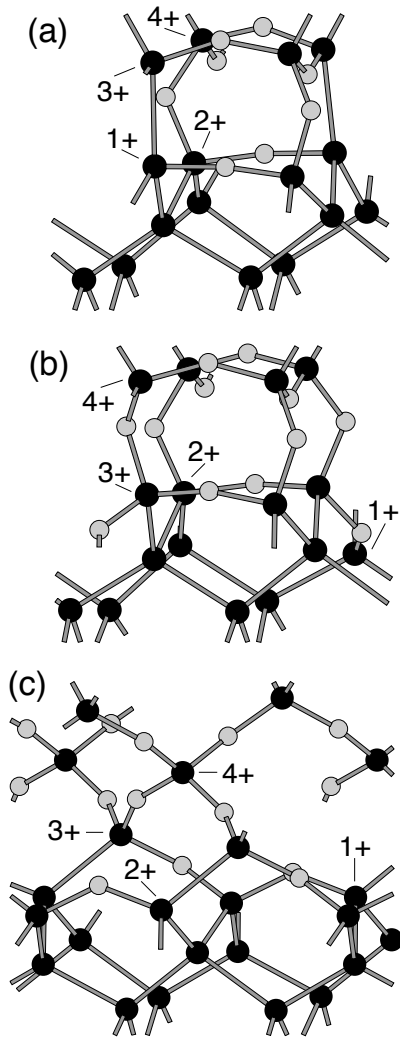


Figure 4. Ball and stick models showing the relaxed positions of several interface structures: (a) Si-Si bond pointing into the oxide, (b) O in the backbond connecting an interface Si atom to the substrate, and (c) β -cristobalite with the construction proposed in Ref. [21] at the interface. The formal Si partial oxidation states are indicated.

states. We therefore did not allow for any unsaturated dangling bond in our interface models. The models are obtained by attaching a crystalline form

of SiO₂, such as tridymite or β -cristobalite, to Si(001). The initial structures obtained in this way are then allowed to relax fully within our theory (see Fig. 4).

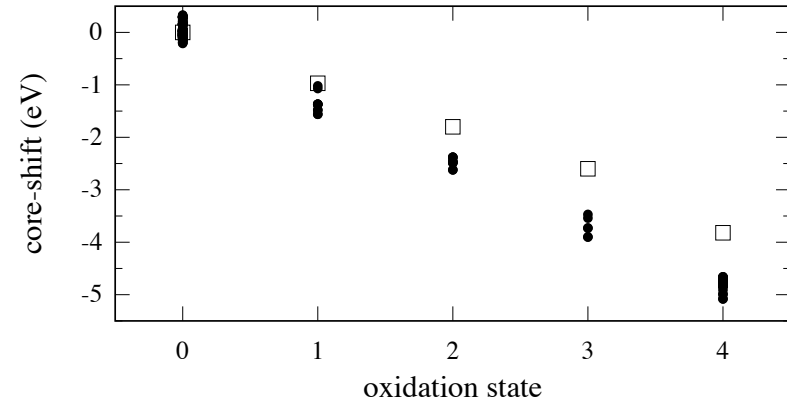


Figure 5. Si 2p core-level shifts at the Si(001)-SiO₂ interface as a function of oxidation state: models (solid circles) and experiment (open squares) from Ref. [18].

In Fig. 5, calculated Si 2p core-level shifts are plotted versus the oxidation state of the silicon atoms to which they belong, and compared to experimental values [18]. Apart from the usual systematic shift to higher binding energies the agreement with experiment is rather good. The calculated Si 2p shifts show a linear dependence on the number of first nearest neighbor oxygen atoms. This result confirms the interpretation based on charge-transfer models. In fact, core-hole relaxation effects account for about 50% of the shifts shown in Fig. 5, but their correction also scales linearly with the number of O neighbors. This increase of the final state effect with O neighbors can be understood as caused by a reduced valence screening in oxidized Si atoms. The large role of core-hole relaxation effects has also been supported experimentally through a careful comparison of photoemission and Auger spectra [22].

6. Nitrated Si(001)-SiO₂ interfaces

The incorporation of a low concentration of nitrogen atoms at the Si(001)-SiO₂ interface has promising applications in the electronic device industry [23, 24, 25]. Further improvement of the dielectric properties of such systems also relies on the availability of detailed microscopic information on the situation of the incorporated N atoms. In this section, we character-

ize these N atoms by establishing a correspondence between their bonding environment and the N $1s$ shifts measured in photoemission experiments.

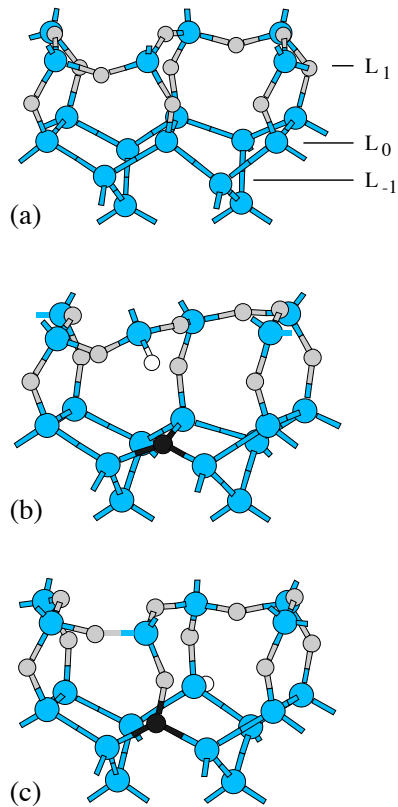


Figure 6. Models of the Si(001)-SiO₂ interface (a) before (from [7]) and after N (black atoms) incorporation, in a (b) N-Si₃ and (c) in a N-Si₂O configuration. L₋₁, L₀ and L₁ label the Si layers. H atoms (white) saturate residual dangling bonds.

The experimental N $1s$ spectra show a broad principal peak (FWHM \approx 1.5 eV), approximately at the same energy as in bulk Si₃N₄, which appears to shift to larger binding energies for samples of increasing oxide thickness [24, 26, 27]. A deeper analysis of the shape of this peak, has led to the recognition of two components [28, 29]. The one closest to the bulk Si₃N₄ energy arises from the interfacial region and is generally attributed to N atoms bonded to three Si atoms (N-Si₃) [28, 29]. The second component, which is shifted by $\Delta=0.85$ eV to larger binding energies [28], mainly results

from N atoms distributed throughout the oxide [28, 29]. The contribution of the latter component increases for thick oxides, accounting for the observed shift of the principal XPS feature. Note, however, that a general consensus has not yet been reached neither on such a decomposition nor on its interpretation. In the presence of this uncertain experimental situation, we use our first-principle approach to explore some plausible bonding configurations.

Using as a starting point of our nitrated interface study one of the Si(001)-SiO₂ interface models obtained previously [see Fig. 6(a)] [7], we generated several nitrated interface models [two of them are shown in Figs. 6(b) and (c)] containing N atoms in different bonding configurations and at varying distances from the interface plane [8].

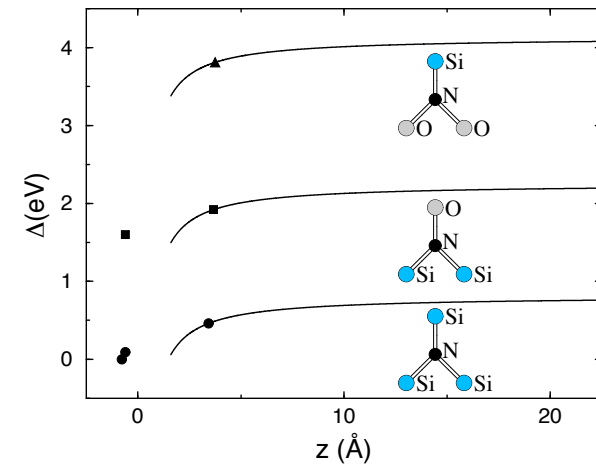


Figure 7. N $1s$ core-level shifts Δ at Si(001)-SiO₂ interfaces calculated for N-Si₃ (circle), N-Si₂O (square), and N-SiO₂ (triangle) configurations at different distances z from the interface. Continuous lines result from classical electrostatics.

N $1s$ shifts for these models were calculated including core-hole relaxation effects and are given in Fig. 7 as a function of the relaxed position z of the N atom with respect to the interface plane [8]. We took as a reference the shift of a N-Si₃ configuration in which the N atom is located most deeply in the Si substrate. From Fig. 7, it is evident that the shifts are strongly affected by first nearest neighbors. The presence of an O nearest neighbor yields shifts to higher binding energies of $\Delta=1.5$ eV with respect to corresponding N-Si₃ configurations. A second oxygen nearest neighbor brings this shift to $\Delta=3.5$ eV. The large separation between the calculated

shifts of N-Si₃ and N-Si₂O configurations virtually rules out the possibility that both configurations contribute to the principal XPS peak.

With increasing distance from the interface the silicon substrate is less effective in screening the core-hole and an increase of the binding energy is observed (Fig. 7) [7]. An extrapolation obtained within classical electrostatics [7] illustrates this effect at large distances in Fig. 7. However, this dependence on distance to the interface only partially explains the observation of two components of different spatial origin in the principal XPS peak. Carr and Buhrman [24] found that as a function of oxide thickness the N 1s peak shifted to larger binding energies by 0.4 eV more than other oxide peaks. We attribute this shift to a chemical change in the second nearest neighbors. In the neighborhood of the substrate the environment around a N-Si₃ center is assumed to be predominantly rich in Si and N atoms [25, 30, 31], whereas an O-rich environment is expected in the oxide. For simulating such environments we studied auxiliary test-molecules in which the central N atom was always kept in a N-Si₃ configuration, while changes in second nearest neighbors were investigated [8]. Calculated shifts in these molecules show that a residual shift of 0.4 eV can indeed be explained in terms of such second nearest neighbor changes. We also explored the possibility of N-Si₂H configurations. The calculated shifts were found to be very close to those of corresponding N-Si₃ configurations. We can therefore not exclude that also N-Si₂H configurations contribute to the principal XPS feature. However, a H concentration of the same order as the N concentration, i.e. of about one monolayer [25, 30, 31], appears unlikely at such interfaces.

In summary, we propose an interpretation of the N 1s photoemission spectra, in which the N atom is found in a *single* first-neighbor configuration (N-Si₃), both in the interfacial region close to the substrate and in the oxide. The dependence of the shape of the principal photoemission feature on oxide thickness is explained in terms of core-hole relaxation and second-nearest neighbor effects. The experimental spectra do not show a peak in correspondence of the calculated shift for an oxygen first-nearest neighbor. This suggests that such configurations are absent at nitrated Si(001)-SiO₂ interfaces.

7. Conclusions

We presented a series of applications in which calculated core-level shifts provided useful support to the interpretation of photoemission spectra. We used a first-principle approach based on density functional theory, which provides a consistent framework both for performing structural relaxations and calculating core-level shifts. The combination of these two features

together with the overall accuracy of the theory, makes of such a scheme a reliable tool to be used in conjunction with experiment. We expect that in the near future theoretical investigations as the ones exposed in this work will routinely be called for to assign unidentified spectral features.

Acknowledgements

We acknowledge fruitful discussions with M.L. Green, E. Garfunkel, E.P. Gusev, and Z.H. Lu.

References

1. L. Pedocchi, N. Russo, and D.R. Salahub, *Phys. Rev. B* **47**, 12992 (1993).
2. A. Pasquarello, M.S. Hybertsen, and R. Car, *Physica Scripta* **T66**, 118 (1996).
3. R. Car and M. Parrinello, *Phys. Rev. Lett.* **55**, 2471 (1985).
4. A. Pasquarello *et al.*, *Phys. Rev. Lett.* **69**, 1982 (1992); K. Laasonen *et al.*, *Phys. Rev. B* **47**, 10142 (1993).
5. E. Pehlke and M. Scheffler, *Phys. Rev. Lett.* **71**, 2338 (1993).
6. We use formulae for the exchange and correlation energy as given in J.P. Perdew and A. Zunger, *Phys. Rev. B* **23**, 5048 (1981).
7. A. Pasquarello, M.S. Hybertsen, and R. Car, *Phys. Rev. Lett.* **74**, 1024 (1995); *Phys. Rev. B* **53**, 10942 (1996).
8. G.-M. Rignanese, A. Pasquarello, J.-C. Charlier, X. Gonze, and R. Car, to be published.
9. W.L. Jolly, K.D. Bomben, and C.J. Eyermann, *Atomic Data and Nuclear Data Tables* **31**, 433 (1984).
10. A. Pasquarello, M.S. Hybertsen, and R. Car, *J. Vac. Sci. Technol. B* **14**, 2809 (1996).
11. M.M. Banaszak Holl and F.R. McFeely, *Phys. Rev. Lett.* **71**, 2441 (1993).
12. S. Lee, S. Makan, M.M. Banaszak Holl, and F.R. McFeely, *J. Am. Chem. Soc.* **116**, 11819 (1994).
13. A. Pasquarello, M.S. Hybertsen, and R. Car, *Phys. Rev. B* **54**, R2339 (1996).
14. Y.J. Chabal and S.B. Christman, *Phys. Rev. B* **29**, 6974 (1984).
15. C.U.S. Larsson, A.S. Flodström, R. Nyholm, L. Incoccia and F. Senf, *J. Vac. Sci. Technol. A* **5**, 3321 (1987).
16. F.J. Himpsel, F.R. McFeely, A. Taleb-Ibrahimi, J.A. Yarmoff and G. Hollinger, *Phys. Rev. B* **38**, 6084 (1988).
17. P.J. Grunthaner, M.H. Hecht, F.J. Grunthaner, and N.M. Johnson, *J. Appl. Phys.* **61**, 629 (1987).
18. Z.H. Lu, M.J. Graham, D.T. Jiang, and K.H. Tan, *Appl. Phys. Lett.* **63**, 2941 (1993).
19. A. Pasquarello, M.S. Hybertsen, and R. Car, *Appl. Phys. Lett.* **68**, 625 (1996).
20. A. Pasquarello, M.S. Hybertsen, and R. Car, *Appl. Surf. Sci.* **104/105**, 317 (1996).
21. I. Ohdomari, H. Akatsu, Y. Yamakoshi, and K. Kishimoto, *J. of Non-Crystal. Solids* **89** 239 (1987); *J. Appl. Phys.* **62** 3751 (1987).
22. A. Iqbal, C.W. Bates Jr., and J.W. Allen, *Appl. Phys. Lett.* **47**, 1064 (1985).
23. M.Y. Hao, W.M. Chen, K. Lai, and C. Lee, *Appl. Phys. Lett.* **66**, 1126 (1995); S.B. Kang, S.O. Kim, J.-S. Byun, and H.J. Kim, *Appl. Phys. Lett.* **65**, 2448 (1994); S.T. Chang, N.M. Johnson, and S.A. Lyon, *Appl. Phys. Lett.* **44**, 316 (1984).
24. E.C. Carr and R.A. Buhrman, *Appl. Phys. Lett.* **63**, 54 (1993).
25. M.L. Green *et al.*, *Appl. Phys. Lett.* **65**, 848 (1994).
26. D.G.J. Sutherland *et al.*, *J. Appl. Phys.* **78**, 6761 (1995).
27. A. Kamath *et al.*, *Appl. Phys. Lett.* **70**, 63 (1997).

28. Z.H. Lu, S.P. Tay, R. Cao, and P. Pianetta, *Appl. Phys. Lett.* **67**, 2836 (1995).
29. S.R. Kaluri and D.W. Hess, *Appl. Phys. Lett.* **69**, 1053 (1996).
30. H.C. Lu *et al.*, *Appl. Phys. Lett.* **69**, 2713 (1996).
31. H.T. Tang *et al.*, *J. Appl. Phys.* **80**, 1816 (1996).